

distances observed for oxamide oxime, for example.³⁵

Summary

The results presented here are of interest in two aspects: (1) The migration of Pt^{IV} from N3 to N4' of a cytosine nucleoside represents a unique example of a linkage isomerization with two intermediates (2 and 3) observed in solution, isolated, and characterized. Usually, and in particular with kinetically labile metal complexes, the mechanism of metal migration can be deduced by indirect methods only. Linkage isomerization processes involving metals bound to a nucleobase, which occasionally have been reported,^{11b,36} could be of considerable biological significance in that the thermodynamically most stable adduct may behave

quite differently from the kinetically favored one. (2) The second point of interest refers to the fact that metal migration from N3 to N4' is coupled with a concomitant reverse migration of a proton, resulting in a change of tautomeric structure of the ligand. While platinum complexes containing a heterocyclic ring in its unusual tautomer form have been described before,^{5,22b} this is the first report of the structure of a rare nucleobase tautomer. As pointed out, the geometry of the free, uncomplexed tautomer can be estimated to a good approximation from the geometry of the complexed tautomer.

Acknowledgment. We thank Dr. Rut Beyerle-Pfnür for providing us with the starting compound 1 and the Deutsche Forschungsgemeinschaft, the Fonds der Chemischen Industrie, and Degussa (loan of K₂PtCl₄) for their support.

Registry No. 1, 101152-06-1; 2, 102149-63-3; 3, 101181-53-7; 5, 103639-09-4; 1-MeC, 1122-47-0.

Supplementary Material Available: Listings of atomic parameters, structural details, and potentiometric titration of 5 (8 pages); listings of observed and calculated structure factors (19 pages). Ordering information is given on any current masthead page.

(35) Endres, H.; Jannack, T.; Prickner, B. *Acta Crystallogr., Sect. B: Struct. Crystallogr. Cryst. Chem.* **1980**, B36, 2230.

(36) (a) Clarke, M. J.; Taube, H. *J. Am. Chem. Soc.* **1975**, 97, 1397. (b) Clarke, M. J. *Inorg. Chem.* **1977**, 16, 738. (c) Lippert, B. *Inorg. Chem.* **1981**, 20, 4326. (d) Scheller, K.; Scheller-Krattiger, V.; Martin, R. B. *J. Am. Chem. Soc.* **1981**, 103, 6833.

(37) As pointed out by one of the referees, the lengthening of C(4)-N(4) in the Ru complex may, at least in part, also be due to a partial double bond character of the Ru^{III}-N(4) bond. Cf.: Clarke, M. J. *Inorg. Chem.* **1980**, 19, 1103.

Reactions of Iron Atoms with Benzene and Cyclohexadienes in Argon Matrices: Iron-Benzene Complexes and Photolytic Dehydrogenation of Cyclohexadiene

David W. Ball, Zakya H. Kafafi, Robert H. Hauge, and John L. Margrave*

Contribution from the Department of Chemistry and Rice Quantum Institute, Rice University, Houston, Texas 77251. Received February 3, 1986

Abstract: Three cyclic C₆ hydrocarbons—benzene (C₆H₆), 1,4-cyclohexadiene, and 1,3-cyclohexadiene (both C₆H₈)—were codeposited with iron atoms in argon matrices at 12–14 K. When iron atoms were cocondensed with benzene, infrared spectra showed the formation of Fe(C₆H₆), Fe(C₆H₆)₂, and Fe₂(C₆H₆) complexes. When iron atoms were codeposited with 1,4-cyclohexadiene, IR spectra showed the formation of Fe(C₆H₈) and Fe₂(C₆H₈) adducts. On photolysis with ultraviolet light the monoiron adduct rearranged to form FeH₂ and benzene in either isolated or adducted states. A similar dehydrogenation reaction was also thought to be observed upon photolysis of the diiron-cyclohexadiene adduct with visible light. 1,3-Cyclohexadiene has been shown to react with iron atoms and dimers in a similar manner. Deuterium isotopic substitution of the three C₆ hydrocarbons was used to obtain confirmatory evidence.

Much recent work has shown that metal atoms, dimers, and small clusters react with other molecules in various surprising ways; matrix isolation spectroscopy has proven to be a powerful tool in studying these reactions.^{1–7} One particular area of research has been the selective activation of bonds by metal atoms, as work in this field has immediate application to catalysis and synthesis and can lead directly to a better understanding of chemical reactivity, which has been targeted recently⁸ as an important area in chemical research. Recent work in our laboratory has included

the study of the codeposition and photolytic reactions of metal atoms with methane,¹ ethylene,⁹ acetylene,¹⁰ diazomethane,¹¹ methanol,¹² and cyclopentadiene.¹³

The results from the iron-cyclopentadiene codeposition study were intriguing: infrared spectra indicated the spontaneous formation of cyclopentadienyliron hydride, the first cyclopentadienyl transition metal hydride detected. One of the reasons for the spontaneous formation of CpFeH (Cp = cyclopentadienyl) was the contribution of aromatic stabilization energy of the Cp anion to the overall ΔH of the reaction ($\Delta H \sim \Delta G$ at low temperatures). It was decided, then, to study the possible reactions of iron atoms with some cyclic C₆ aromatic or near-aromatic

(1) Billups, W. E.; Konarski, M. M.; Hauge, R. H.; Margrave, J. L. *J. Am. Chem. Soc.* **1980**, 102, 7393.

(2) Forstmann, F.; Kolb, D. M.; Leutloff, D.; Schulze, W. *J. Chem. Phys.* **1977**, 66, 2806.

(3) Kasai, P. A.; McLeod, D. J. *J. Chem. Phys.* **1971**, 55, 1566.

(4) Klabunde, K.; Tanaka, Y. *J. Am. Chem. Soc.* **1983**, 105, 3544.

(5) Moskovits, M.; Ozin, G. *Crycochemistry*; John Wiley and Sons: New York, 1976.

(6) Kafafi, Z. H.; Hauge, R. H.; Fredin, L.; Billups, W. E.; Margrave, J. L. *J. Chem. Soc., Chem. Commun.* **1983**, 1230.

(7) Burdett, J. K.; Turner, J. J. *J. Chem. Soc., Chem. Commun.* **1971**, 885.

(8) Pimentel, G. C., chairman *Opportunities in Chemistry*; U.S. National Academy of Sciences: Washington, D.C., 1985.

(9) Kafafi, Z. H.; Hauge, R. H.; Margrave, J. L. *J. Am. Chem. Soc.* **1985**, 107, 7550.

(10) Kline, E. S.; Kafafi, Z. H.; Hauge, R. H.; Margrave, J. L. *J. Am. Chem. Soc.* **1985**, 107, 7559.

(11) Chang, S.-C.; Kafafi, Z. H.; Hauge, R. H.; Billups, W. E.; Margrave, J. L. *J. Am. Chem. Soc.* **1985**, 107, 1447.

(12) Park, M.; Kafafi, Z. H.; Hauge, R. H.; Margrave, J. L. *J. Chem. Soc., Chem. Commun.* **1985**, 1570.

(13) Ball, D. W.; Kafafi, Z. H.; Hauge, R. H.; Margrave, J. L. *Inorg. Chem.* **1985**, 24, 3708.

hydrocarbons: benzene, 1,3-cyclohexadiene, and 1,4-cyclohexadiene.

The cocondensation of iron and benzene has been studied previously with varying concentrations and temperatures.¹⁴⁻¹⁹ However, no photolysis studies had been performed. The iron-benzene system was first studied by Timms,¹⁴ who reported a complex of unknown stoichiometry. Efner et al.¹⁵ studied iron and benzene in argon matrices (molar ratio of benzene to argon = 4:100) and reported infrared data for a species that they determined to be $\text{Fe}(\text{C}_6\text{H}_6)$. Aleksanyan and Kurtikyan¹⁶ and Skell et al.¹⁷ also studied the codeposition of iron and benzene in neat matrices. Both research groups assigned the new infrared absorptions to an $\text{Fe}(\text{C}_6\text{H}_6)_2$ complex. Skell¹⁷ even made a direct comparison between his results and the results of Efner, neglecting the difference in matrix composition. More recently, Morand and Francis¹⁸ studied iron-benzene cocondensation and assigned new peaks in the visible spectrum to a $(\eta^6\text{-C}_6\text{H}_6)(\eta^4\text{-C}_6\text{H}_6)\text{Fe}$ complex. Though they did point out the difference in matrix composition between their work and previous work, they presented little infrared data for direct comparison.

Parker and Peden¹⁹ studied iron and benzene codeposited in krypton matrices at 7 K. By carrying out concentration studies of both reactants, they used Mossbauer spectroscopy to unambiguously identify many iron-benzene complexes, including an $\text{Fe}(\text{C}_6\text{H}_6)$ complex and several $\text{Fe}(\text{C}_6\text{H}_6)_2$ complexes. However, since they did use Mossbauer spectra, their results cannot be used to rectify the schism that seems apparent in the assignment of infrared absorptions to these two species. The work presented here indicates that both $\text{Fe}(\text{C}_6\text{H}_6)$ and $\text{Fe}(\text{C}_6\text{H}_6)_2$ exist and are identifiable with infrared spectroscopy. The formation of either species is directly dependent on the concentration of benzene in the matrix. It is also shown that a possible problem in earlier studies in making the assignments might have been the aggregation of benzene at even low matrix concentrations.

Cyclohexadiene has been deposited in argon matrices as far back as 1971, when Boikess et al. studied the photolytic isomerization of 1,3-cyclohexadiene to 1,3,5-hexatrienes.²⁰ Morand and Francis¹⁸ studied the cocondensation of iron with 1,3-cyclohexadiene, but these matrices were neat or not very dilute (10% solution in methylcyclohexane). They reported a disproportionation reaction to form benzene and cyclohexene at high iron concentrations. They suggested that the disproportionation reaction was due to iron clusters rather than a bis(cyclohexadiene)iron complex. Skell has also studied the reactions of iron atoms with 1,3-cyclohexadiene at 77 K.²¹ He, too, reported a catalytic disproportionation of 1,3-cyclohexadiene to cyclohexene and benzene and has produced the complex (benzene)(1,3-cyclohexadiene)iron(0).

We present here a photolytic reaction between iron atoms or dimers and cyclohexadiene (both isomers) where the cyclohexadiene ring is dehydrogenated by iron atoms to form benzene and FeH_2 . Spectra characteristic of FeH_2 , $\text{Fe}(\text{C}_6\text{H}_6)$, and a new species $\text{H}_2\text{Fe}(\text{C}_6\text{H}_6)$ have been identified in the case of the monoiron-cyclohexadiene photoreaction.

Experimental Section

A complete description of the matrix isolation apparatus has been published.²² The deposition surface was a polished rhodium-plated copper block cooled to 12–14 K with a closed cycle helium refrigerator. The molar ratios of the reactants were measured by utilizing a quartz

crystal microbalance with a frequency of approximately 6 MHz. The iron was obtained from Aesar (99.98%) and was deposited from an alumina crucible wrapped in tantalum foil which was resistively heated to the temperature range 1100–1400 °C. Temperatures were measured by viewing the tantalum furnace with a microoptical pyrometer from the Pyrometer Instrument Co.; no emissivity corrections were made. Benzene (Aldrich, Spectrophotometric Grade, 99+%), benzene- d_6 (Aldrich, 99.5%), 1,3-cyclohexadiene (Aldrich, 96%), and 1,4-cyclohexadiene (Aldrich, 97%) were dried over molecular sieves and used without further purification.

Deuterated cyclohexadienes were synthesized in the laboratory. Five grams of 1,4-cyclohexadiene were mixed in 50 mL of distilled pentane, and the resultant solution was vigorously stirred with a solution of 0.8 g of potassium *tert*-butoxide in 25 g of $\text{Me}_2\text{SO}-d_6$ for 4 h. At the end of this time the Me_2SO layer was drawn off and replaced by a fresh $\text{KOtBu}/\text{Me}_2\text{SO}-d_6$ solution. After 4 h of stirring, the Me_2SO layer was drawn off and the pentane solution was distilled to remove the pentane (bp 36 °C). Approximately 5 mL of cyclohexadiene was left over after distillation and separated into 1,3-cyclohexadiene- d_8 and 1,4-cyclohexadiene- d_8 (1,3:1,4 = ~5:1) by preparative gas chromatography. NMR and IR spectra confirmed the purity of the final products.

Iron and benzene or iron and cyclohexadiene were codeposited in excess argon onto the rhodium-plated copper surfaces. The depositions lasted either 15 or 30 min. After deposition, the surface was rotated 180° and the infrared spectrum was measured with an IBM IR-98 Fourier transform infrared spectrophotometer.

Photolysis studies were also performed. Matrices were irradiated after deposition for 30 min with a 100-W medium-pressure short-arc mercury lamp. A water/Pyrex filter and various Corning long-pass cutoff and band-pass filters were used for wavelength-dependent photolysis studies.

Results and Discussion

The matrix infrared spectra of benzene, 1,3-cyclohexadiene (1,3-CHD), 1,4-cyclohexadiene (1,4-CHD), and the three perdeuterated species have been measured and are shown in Figures 1-S and 2-S of the supplementary material. The fundamental vibrations of these matrix-isolated species were verified by comparison with earlier work on benzene,²³⁻²⁵ 1,3-CHD,^{20,26} and 1,4-CHD.²⁷

Iron + Benzene. Iron atoms were codeposited with low concentrations of benzene and benzene- d_6 , resulting in the formation of new infrared absorptions that grew monotonically with increasing iron concentration. These new peaks were assigned to an iron atom adducting to benzene. At high iron concentrations (ca. 10 parts per thousand of argon), a second set of peaks was noted that grew at a rate different from that of the first set of peaks; these peaks were assigned to a diiron adduct with benzene. A selected region of the infrared spectra showing the iron concentration study is given in Figure 1a.

A plot of the ratio of the absorbance of the diiron adduct to the absorbance of the monoiron adduct vs. iron concentration is given in Figure 1b. It has been shown that, for a metal M reacting with a ligand L in a cryogenic matrix, the amount of ligated metal cluster M_xL formed in the matrix relative to the ligated metal atom ML is:²⁸

$$[\text{M}_x\text{L}]/[\text{ML}] \propto [\text{M}]_0^{x-1} \quad (1a)$$

In this case, M = Fe and x = 2:

$$[\text{Fe}_2\text{L}]/[\text{FeL}] = k[\text{Fe}]_0 \quad (1b)$$

From substituting the Beer-Lambert law one gets (L = C_6H_6)

$$\frac{A_{\text{Fe}_2\text{L}}/\epsilon_{\text{Fe}_2\text{L}}b}{A_{\text{FeL}}/\epsilon_{\text{FeL}}b} = k[\text{Fe}]_0 \quad (1c)$$

$$A_{\text{Fe}_2\text{L}}/A_{\text{FeL}} = k(\epsilon_{\text{Fe}_2\text{L}}/\epsilon_{\text{FeL}})[\text{Fe}]_0 \quad (1d)$$

which is an equation for a straight line. Since the points plotted in Figure 1b yield a straight line (correlation coefficient = 0.96),

(23) (a) Herzberg, G. H. *Infrared and Raman Spectra of Polyatomic Molecules*; Van Nostrand Reinhold: Scarborough, Ontario, Canada, 1945; pp 364–365. (b) Spoliti, M.; Cesaro, S. N.; Grosso, V. *Spectrochim. Acta A* 1976, 32, 145.

(24) Brown, K. G.; Person, W. B. *Spectrochim. Acta A* 1978, 34, 117.

(25) Mair, R. D.; Hornig, D. F. *J. Chem. Phys.* 1949, 17, 1236.

(26) DiLauro, C.; Neto, N.; Califano, S. *J. Mol. Struct.* 1969, 3, 219.

(27) Stidham, H. D. *Spectrochim. Acta* 1965, 21, 23.

(28) Reference 5, p 436.

(14) Timms, P. L. *J. Chem. Soc., Chem. Commun.* 1969, 1033.
(15) Efner, H. F.; Tevault, D. E.; Fox, W. B.; Smardzewski, R. R. *J. Organomet. Chem.* 1978, 146, 45.

(16) Aleksanyan, V. T.; Kurtikyan, T. S. *Koord. Khim.* 1977, 3, 1548.

(17) Shobert, A. L.; Hisatsume, L. C.; Skell, P. S. *Spectrochim. Acta A* 1984, 40, 609.

(18) Morand, P. D.; Francis, C. G. *Organometallics* 1985, 4, 1653.

(19) Parker, S. F.; Peden, C. H. F. *J. Organomet. Chem.* 1984, 272, 411.

(20) Datta, P.; Goldfarb, T. D.; Boikess, R. S. *J. Am. Chem. Soc.* 1971, 93, 5189.

(21) Williams-Smith, D. L.; Wolf, L. R.; Skell, P. S. *J. Am. Chem. Soc.* 1972, 94, 4042.

(22) Hauge, R. H.; Fredin, L.; Kafafi, Z. H.; Margrave, J. L. *Appl. Spectrosc.* 1986, 40, 588.

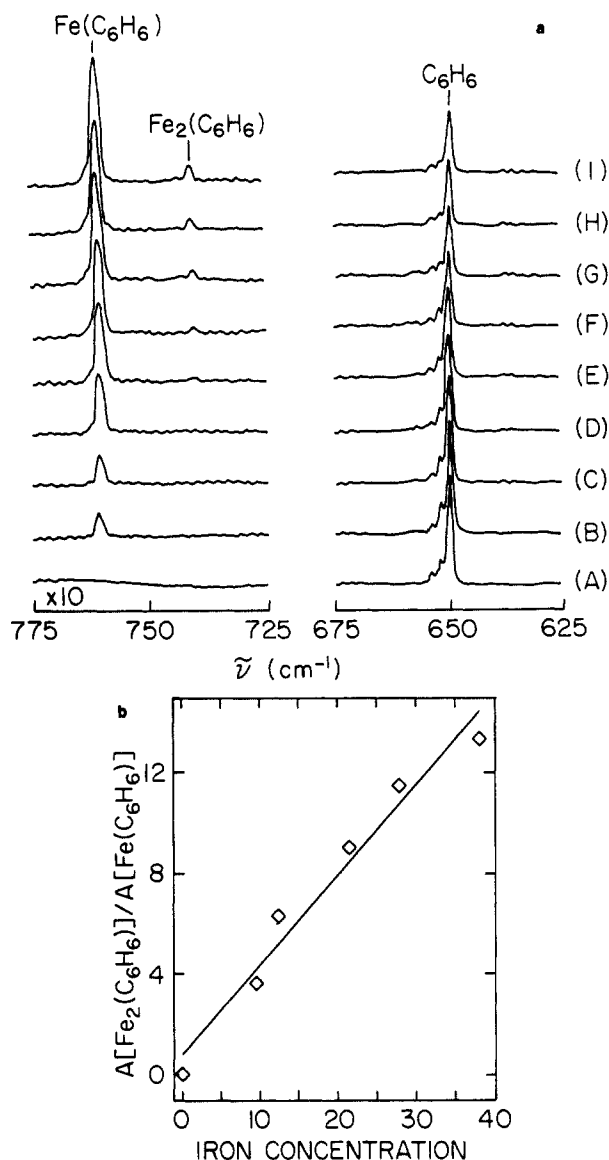


Figure 1. (a) Codeposition of iron and benzene in argon matrices: (A) shows regions of the benzene "blank" spectrum; (B–I) show the same regions with increasing concentrations of iron. Molar ratio of benzene to argon is constant at 3.1:1000. The iron to argon ratios are (B) 0.9:1000, (C) 1.9:1000, (D) 4.4:1000, (E) 9.6:1000, (F) 12.3:1000, (G) 21.4:1000, (H) 27.9:1000, (I) 38.1:1000. (b) Plot of the ratio of the absorbance of the diiron–benzene adduct to that of the monoiron–benzene adduct vs. the concentration of iron in the matrix. The straight-line behavior of the graph confirms that the adduct at higher Fe concentrations is due to $\text{Fe}_2(\text{C}_6\text{H}_6)$ (see text and references cited therein).

this confirms the identity of the $\text{Fe}_2(\text{C}_6\text{H}_6)$ adduct.

The frequencies of the monoiron adduct peaks agree very well with those reported by Efner et al.,¹⁵ who assigned the new absorptions to an $\text{Fe}(\text{C}_6\text{H}_6)$ complex. This assignment, however, seems to be in contradiction with the assignments by Skell¹⁷ and Aleksanyan,¹⁶ who favor an $\text{Fe}(\text{C}_6\text{H}_6)_2$ complex.

A concentration study in benzene supplied the resolution to this apparent contradiction. A relevant portion of this study is shown in Figure 2. In Figure 2B, one can see the formation of new peaks as iron was cocondensed with benzene. As the benzene concentration was increased, the peak at 760.8 cm^{-1} decreased while the peak at 717.6 cm^{-1} increased. The peak at 717.6 cm^{-1} was present for iron in a neat benzene matrix (Figure 2F) while in the same spectrum there was no sign of the absorption at 760.8 cm^{-1} . A spectrum of a matrix containing a high concentration of benzene but no iron did not show the peak at 717.6 cm^{-1} , verifying that this peak is due to an iron–benzene adduct and is not a benzene aggregate absorption. The peak at 717.6 cm^{-1} and related ab-

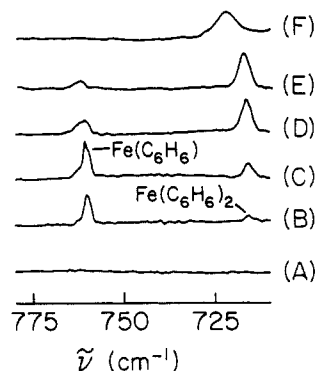


Figure 2. Benzene and iron codeposition study in argon matrices: (A) shows a region of the benzene "blank" spectrum; (B–F) show the same region but with iron codeposited with the benzene. Molar ratio of iron to argon is constant at 4.9:1000. The benzene concentrations are (B) 5.1:1000, (C) 7.8:1000, (D) 18:1000, (E) 50:1000, (F) neat benzene plus same amount of iron. Note that only $\text{Fe}(\text{C}_6\text{H}_6)_2$ is present in neat matrices.

Table I. Infrared Absorptions of Various Iron–Benzene Complexes Identified in Cryogenic Argon Matrices (in cm^{-1})

$\text{Fe}(\text{C}_6\text{H}_6)$	$\text{Fe}(\text{C}_6\text{H}_6)_2$	$\text{Fe}_2(\text{C}_6\text{H}_6)$	$\text{Fe}(\text{C}_6\text{D}_6)$	$\text{Fe}(\text{C}_6\text{D}_6)_2$
678.4 (m)	664.1 (m)	740.5 (m)	583.6 (s)	533.7 (m)
760.8 (s)	715.7 (s)	992.4 (w)	785.9 (m)	796.2 (m)
812.4 (m)	967.6 (w)	1010.0 (w)	907.0 (w)	
952.7 (w)	1441.0 (m)	1429.0 (w)	1257.6 (w)	
983.6 (w)				
1421.0 (w)				

sorptions agree very well with those reported by Skell¹⁷ and Aleksanyan.¹⁶

The immediate conclusion from this study is that the peak at 760.8 cm^{-1} and related absorptions are due to the monobenzene complex, $\text{Fe}(\text{C}_6\text{H}_6)$. The fact that these peaks were seen at the lowest concentrations of Fe and benzene studied indicates that these absorptions are not due to an $\text{Fe}_n(\text{C}_6\text{H}_6)$, $n > 1$, species; a complex of this type is identified at higher concentrations of iron. The peak at 717.6 cm^{-1} and related absorptions are then due to the dibenzene complex, $\text{Fe}(\text{C}_6\text{H}_6)_2$. These assignments are listed in Table I. This conclusion also implies that the interpretation of previous individual works were correct but that the comparisons of some of the earlier results should not have been made due to the differing concentrations of benzene studied. Comparisons of the absorptions for the $\text{Fe}(\text{C}_6\text{H}_6)$ and $\text{Fe}(\text{C}_6\text{H}_6)_2$ adducts with earlier results can now be made directly and are presented in Table IIA,B. With these tables as evidence we can firmly state that both $\text{Fe}(\text{C}_6\text{H}_6)$ and $\text{Fe}(\text{C}_6\text{H}_6)_2$ are present in cryogenic matrices and identifiable with infrared spectroscopy.

A close inspection of the spectra obtained in this study with data presented by Efner¹⁵ and Aleksanyan¹⁶ showed that the two earlier studies reported frequencies for the iron–benzene complex that are due instead to benzene aggregates; these absorptions are noted in Table IIA,B. Since full spectral series were not included with the above references, only possible misinterpretation can be suggested. It is interesting to note that these aggregate absorptions are detectable even at benzene concentrations $< 0.5\%$; hence, complete isolation of benzene molecules is not attained at even that low level. This fact may have contributed to earlier disagreement in the interpretation of earlier studies.

Photolysis studies were also conducted on the dilute iron–benzene matrices. Selected matrices were photolyzed for 30 min with a medium-pressure mercury-arc lamp and various Corning filters ($\lambda > 500\text{ nm}$, $\lambda > 400\text{ nm}$, and $220\text{ nm} < \lambda < 380\text{ nm}$). In all cases, no new peaks were seen that could be attributed to the formation of an oxidative addition product. This result was surprising (and disappointing) in light of the fact that some transition-metal complexes will undergo an oxidative addition reaction into an aromatic C–H bond:²⁹

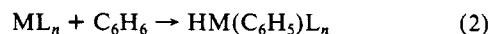


Table II. Comparison of Reported Frequencies (cm^{-1}) of the $\text{Fe}(\text{C}_6\text{H}_6)$ Species in Argon Matrices with the $\text{Fe}(\text{C}_6\text{H}_6)_2$ Species in Neat Matrixes

(A) $\text{Fe}(\text{C}_6\text{H}_6)$ Species					
this work	Efner et al. ^{14a}	this work	Efner et al. ^{14a}		
	366	893.4	983		
678.1			993 ^b		
746.3			1010 ^b		
760.8	762		1179 ^b		
812.4	812		1246 ^b		
952.7	953		1392 ^b		
		1421.0	1430		
(B) $\text{Fe}(\text{C}_6\text{H}_6)_2$ Species					
this work	Aleksa- nyan et al. ¹⁵	Skell et al. ¹⁶	this work	Aleksa- nyan et al. ¹⁵	Skell et al. ¹⁶
	609	600	967.6	968	965
664.1				978	
	685			989	
715.7	709	715		1011 ^c	
	725			1035 ^c	
	780	775		1148 ^c	
	859	855		1175 ^c	1175 ^c
	930			1310 ^c	
				1412	
			1441.0	1438	1435
				1478 ^c	

^a Molar ratio of C_6H_6 to Ar = 25:1000. ^b These peaks are assigned to benzene aggregate modes in this study. ^c These peaks are assigned to benzene aggregate modes in this study.

The lack of similar reactivity for these iron-benzene matrix cases may be due to the effective atomic number (EAN) rule: as a π -complex, an iron in $\text{Fe}(\text{C}_6\text{H}_6)$ has an EAN of 32, whereas for the insertion product HFeC_6H_5 , the iron atom has an EAN of 28. Hence the π -complex is more coordinatively saturated and, by the general principles of the EAN rule, presumably more stable.

We balk at trying to satisfy the EAN rule for the bis(benzene)iron complex; Parker and Peden¹⁹ did this in part in their Mossbauer study and Morand and Francis¹⁸ described their bis(benzene) complex as $\eta^6\text{-}\eta^4$. It might well be the case that the two benzene ligands are coordinatively inequivalent, but the vibrational spectra presented in this study cannot be used as evidence for either a $\eta^6\text{-}\eta^4$ or a $\eta^6\text{-}\eta^6$ coordination complex.

It should be mentioned, though, that matrices containing a high concentration of benzene with iron displayed a distinct green color, which is noteworthy because iron matrices generally have reddish-brown colors. Now, it is known¹³ that ferrocene, FeCp_2 ($\text{Cp} = \text{C}_5\text{H}_5^-$), is green in a cryogenic argon matrix (the color change from the characteristic bright orange to green has been attributed to a solid state phase change that occurs at 164 K). A similar color implies a similar visible spectrum, which in turn may imply a similar electronic structure between ferrocene and the $\text{Fe}(\text{C}_6\text{H}_6)_2$ complex, i.e., an iron atom sandwiched between two equivalent π -electron clouds. Ipso facto, the green matrix color in these studies may indicate the formation of a $\eta^6\text{-}\eta^6$ -type coordination. Further work is indicated to explore this possibility.

Iron + Cyclohexadiene. Iron was codeposited with 1,3-CHD and 1,4-CHD in excess argon. For each isomer CHD, a new set of absorptions appeared that increased monotonically with increasing iron concentration; these new peaks were assigned to iron-CHD adducts. It can be seen in Figure 3 that some of the adduct peaks appear at the lowest concentration of iron, while other peaks were not seen until the matrix concentration of iron was high. On the basis of this evidence, the two groups of peaks were assigned to a monoiron-CHD adduct and a diiron-CHD adduct, respectively (cf. benzene). Similar assignments were made in the codeposition of iron and deuterated CHD. The infrared absorptions of these adducts are listed in Tables III and IV. The

Table III. Infrared Absorptions (cm^{-1}) of the Iron-1,4-Cyclohexadiene Codeposition Products

$\text{Fe}(\text{C}_6\text{H}_8)$	$\text{Fe}_2(\text{C}_6\text{H}_8)$	$\text{Fe}(\text{C}_6\text{D}_8)$	$\text{Fe}_2(\text{C}_6\text{D}_8)$
1427.8 (m)	851.2 (vw)	1054.6 (m)	1269.4 (m)
2819.9 (m)	1158.3 (w)	2061.8 (m)	1400.3 (w)
	1168.9 (w)		1825.3 (w)
	1174.7 (w)		1827.0 (w)
	1187.0 (w)		2016.0 (m)
	1195.2 (w)		2020.6 (m)
	1377.9 (w)		2030.0 (m)
	1391.6 (w)		
	1398.6 (w)		
	1413.8 (w)		
	2782.3 (w)		

Table IV. Infrared Absorptions (cm^{-1}) of the Iron-1,3-Cyclohexadiene Codeposition Products

$\text{Fe}(\text{C}_6\text{H}_8)$	$\text{Fe}_2(\text{C}_6\text{H}_8)$	$\text{Fe}(\text{C}_6\text{D}_8)$	$\text{Fe}_2(\text{C}_6\text{D}_8)$
591.3 (w)	642.2 (w)	816.2 (s)	575.4 (m)
722.5 (m)	835.8 (w)	1452.4 (m)	1159.0 (w)
765.8 (w)	1268.5 (w)	1618.0 (m)	1375.0 (w)
771.6 (w)	1382.5 (vw)		1376.2 (w)
905.2 (m)	1811.6 (vw)		2045.9 (w)
940.4 (w)	1827.0 (vw)		
1264.4 (m)	2015.7 (w)		
1482.7 (m)	2061.8 (w)		
1702.1 (m)	2768.1 (w)		
1722.6 (w)			
1740.0 (w)			
3099.8 (w)			

Table V. Comparison of the Photoproduct Infrared Absorptions (cm^{-1}) for the Visible-Photolyzed Fe-1,3-CHD and Fe-1,4-CHD in Argon Matrices

Fe + 1,3-CHD	Fe + 1,4-CHD	Fe + 1,3-CHD- d_8	Fe + 1,4-CHD- d_8
	766.3 (w)	1200.0 (m)	1200.0 (m)
985.5 (w)	986.5 (w)		1208.9 (w)
1665.7 (m)	1665.7 (m)	1216.1 (w)	1216.4 (w)
		1221.9 (w)	

Table VI. Comparison of the Photoproduct Infrared Absorptions (cm^{-1}) for the UV-Photolyzed Fe-1,3-CHD and Fe-1,4-CHD in Argon Matrices

Fe + 1,3-CHD	Fe + 1,4-CHD	Fe + 1,3-CHD- d_8	Fe + 1,4-CHD- d_8
696.4 (w)	696.4 (w)	584.6 (w)	584.6 (w)
760.8 (m)	760.1 (m)	915.1 (vw)	915.1 (vw)
914.6 (w)	907.0 (w)	1030.8 (w)	
1477.1 (m)	1477.7 (m)	1174.9 (w)	1174.7 (w)
1627.4 (w)	1627.4 (w)	1179.3 (w)	1178.8 (w)
1631.2 (w)	1631.2 (w)	1183.6 (w)	
1634.4 (w)	1634.4 (w)	1188.4 (w)	
1657.5 (w)	1656.8 (w)	1194.2 (w)	1194.4 (w)
1660.9 (m)	1660.9 (m)	1196.6 (w)	1197.1 (w)

absorptions for the iron-1,3-CHD adducts bear little resemblance to those reported by Morand and Francis,¹⁸ who performed this experiment in neat matrices.

On photolysis of the codeposition matrices with light of $\lambda > 500$ nm, a new set of peaks was seen to grow with concomitant decrease of those peaks assigned to the Fe_2 -CHD adduct (see Figure 4). Photolysis with light of $\lambda > 400$ nm caused an increase of these diiron photoproduct peaks.

On photolysis with UV light ($220 \text{ nm} < \lambda < 380 \text{ nm}$), a second new set of absorptions was seen while at the same time the absorptions assigned to the monoiron-CHD adduct decreased. These new peaks are attributed to the formation of a monoiron photoproduct. Tables V and VI list the absorptions of the diiron and the monoiron photoproducts, respectively, of 1,4-CHD and 1,3-CHD. These new absorptions did not correspond to those reported by Boikess et al.,²⁰ indicating that no isomerization of the CHDs themselves had occurred.

(29) See, for example: Rausch, M. D.; Gastinger, R. G.; Gradner, S. A.; Brown, R. K.; Wood, J. S. *J. Am. Chem. Soc.* 1977, 99, 7870.

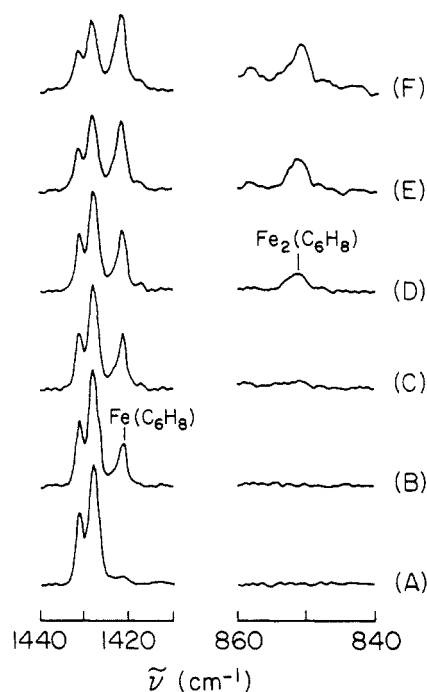


Figure 3. Codeposition of iron and 1,4-cyclohexadiene in argon matrices. Here it is shown how the iron adducts were identified on the basis of the rate of peak growth; the diiron adduct is not seen until higher concentrations of iron were present in the matrix. Molar ratio of reactants to matrix are 1,4-CHD:Fe:Ar = (A) 3.6:0:1000, (B) 3.6:1.4:1000, (C) 3.6:2.3:1000, (D) 3.6:3.5:1000, (E) 3.6:6.5:1000, (F) 3.6:10.5:1000.

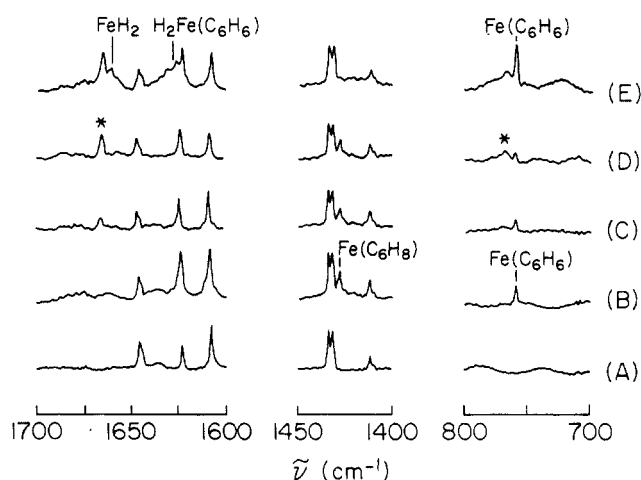


Figure 4. Photolysis study of 1,4-CHD + Fe in argon matrices: (A) 1,4-CHD:Fe:Ar = 3.6:0:1000, (B) 1,4-CHD:Fe:Ar = 3.6:10.2:1000, (C) same as B, photolyzed with light $\lambda > 500$ nm; (D) same as B, photolyzed with light $\lambda > 400$ nm; (E) same as B, photolyzed with UV light, $200 \text{ nm} < \lambda < 380 \text{ nm}$. Note in spectrum B the appearance of the $\text{Fe}(\text{C}_6\text{H}_6)$ absorption; this is due to a small amount of benzene impurity in the 1,4-CHD sample (cf. Figure 3). An asterisk indicates a product resulting from the photorearrangement of $\text{Fe}_2(\text{C}_6\text{H}_8)$.

The identity of the monoiron photoproduct will be discussed first. Figure 4 shows spectra of the photolyses of Fe/1,4-CHD matrices. In Figure 4B, the peak at 760.8 cm^{-1} is due to the iron-benzene 1:1 complex, as described above (benzene is present in 1,4-CHD in small quantities as an impurity). On photolysis with UV light (Figure 4E), this absorption increased in a manner inconsistent with the photolytic behavior of the $\text{Fe}(\text{C}_6\text{H}_6)$ complex; it must have resulted from a photoreaction of the $\text{Fe}(\text{C}_6\text{H}_8)$ adduct. Since there was benzene already present in the matrix, substantiation of this idea was desired. Support was obtained from the photolysis study of iron codeposited with 1,4-CHD- d_8 , which is shown in Figure 5. Infrared spectra of the matrix before photolysis (Figure 5A) show no benzene- d_6 or $\text{Fe}(\text{C}_6\text{D}_6)$ present (cf.

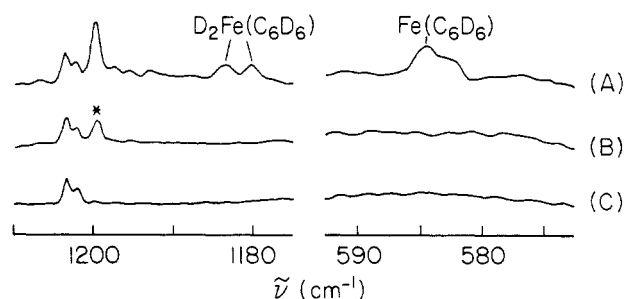


Figure 5. Photolysis study of 1,4-CHD- d_8 + Fe in argon matrices: (A) 1,4-CHD- d_8 :Fe:Ar = 4.7:14.3:1000, (B) same as A, photolyzed with light $\lambda > 500 \text{ nm}$; (C) same as A, photolyzed with UV light, $200 \text{ nm} < \lambda < 380 \text{ nm}$. An asterisk indicates a product resulting from the photorearrangement of $\text{Fe}_2(\text{C}_6\text{D}_8)$.

Scheme I

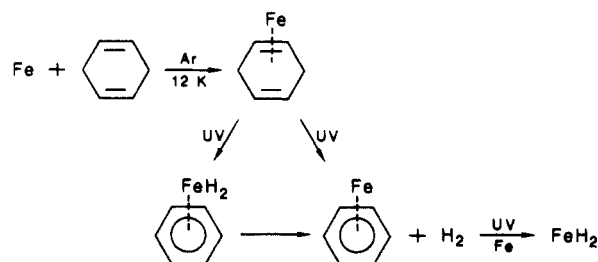


Table 1, Figure 2), but upon photolysis with UV light (Figure 5C) a new peak appeared at 584.8 cm^{-1} , which corresponds to the strongest absorption of the $\text{Fe}(\text{C}_6\text{D}_6)$ complex (cf. Table I). Simultaneously, the $\text{Fe}(\text{C}_6\text{D}_8)$ adduct absorptions decreased (not shown). It is therefore concluded that benzene is being formed by some UV-photolyzed rearrangement of the $\text{Fe}(\text{1,4-C}_6\text{H}_8)$ adduct.

In order for CHD to be dehydrogenated to benzene, it must lose two hydrogens (or deuteriums). Evidence that this process has indeed happened is seen in Figure 4 in the spectral range $1700\text{--}1600 \text{ cm}^{-1}$ and in Figure 5 in the spectral range $1225\text{--}1150 \text{ cm}^{-1}$ for the deuterated CHD. These are the regions for the Fe-H (or Fe-D) stretch. UV photolysis of iron-CHD matrices causes the growth of a plethora of peaks in this region. Iron dihydride, FeH_2 , is known³⁰ to absorb at 1660.9 cm^{-1} in argon matrices; inspection of the UV-photolyzed Fe/ C_6H_8 matrices (Figure 4E) shows a photoproduct peak that corresponds to this absorption. The same correspondence could not be seen in the deuteration study since the FeD_2 absorption is at 1205 cm^{-1} which will be hidden under the C_6D_8 peak.

It can therefore be conclusively stated that *iron atoms photolytically dehydrogenate 1,4-cyclohexadiene to form $\text{Fe}(\text{C}_6\text{H}_6)$ and hydrogen*. Hydrogen may further photoreact with Fe and form iron dihydride.

Other photoproduct peaks in the $1700\text{--}1625\text{-cm}^{-1}$ region are assigned to Fe-H stretches, which are shifted to the $1200\text{--}1150\text{-cm}^{-1}$ region upon deuteration. We believe that these absorptions are due in part to FeH_2 complexed to benzene, which can be considered a (benzene)dihydridoiron complex.

FeH_2 , $\text{Fe}(\text{C}_6\text{H}_6)$, and $\text{H}_2\text{Fe}(\text{C}_6\text{H}_6)$ are all products of the $\text{Fe}(\text{C}_6\text{H}_8)$ photorearrangement. This is not surprising when one considers the fact that hydrogen is one of the few species known to diffuse through a solid cryogenic matrix. Hydrogens that are abstracted from the CHD ring can either bond to the adducting iron atom to form $\text{H}_2\text{Fe}(\text{C}_6\text{H}_6)$ or diffuse through the matrix and react with an isolated iron atom to form FeH_2 (of course, the hydrogens may remain as isolated H_2 or diffuse out of the matrix entirely; either way, they would not show any infrared absorptions). These different reaction pathways are illustrated in Scheme I. This scheme completely explains the formation of all of the species known to be formed in the photoreaction between Fe atoms and

(30) Rubinovitz, R. L.; Nixon, E. R. *J. Phys. Chem.* **1986**, *90*, 1940.

1,4-CHD.

There is no need to go through a similar analysis for the Fe-(1,3-CHD) UV photoproduct. Comparison of Tables V and VI shows that the UV photoproducts for both CHD isomers have identical infrared absorptions and hence are the same.

The identity of the diiron photoproduct should be mentioned. The diiron-CHD adduct rearranges upon visible light photolysis to form a new product (see Figures 3 and 4 and Tables III-V). While the nature of this photoproduct is uncertain, it is thought that the photoreaction is either a dehydrogenation or a C-H bond insertion/oxidative addition. The expected products for the dehydrogenation reaction are benzene and diiron dihydride (Fe_2H_2), while the C-H bond insertion reaction would yield $\text{HFe}_2\text{C}_6\text{H}_7$.

If the photolysis causes dehydrogenation to occur, one would expect $\text{Fe}_2(\text{C}_6\text{H}_6)$ to be one product (just like $\text{Fe}(\text{C}_6\text{H}_6)$ is a product for the monoiron dehydrogenation). The absorptions for the $\text{Fe}_2(\text{C}_6\text{H}_6)$ adduct are given in Table I, and comparison with the diiron adduct photoproducts from Table V shows marginal agreement. Since the vibrational spectrum of Fe_2H_2 , another expected product akin to FeH_2 , is not yet known, a conclusion labeling the reaction as dehydrogenation, based on this evidence alone, would be premature.

On the other hand, if the photoproduct were of the C-H bond insertion type, one would expect to see an Fe-H stretch among the new absorptions; few absorptions in the Fe-H stretching mode have been identified in the photoproduct spectrum. One would also expect to see other bands due to the lowering of molecular symmetry coincident with dimer insertion into the C-H bond. The spectroscopic evidence obtained so far just does not seem to provide an adequate number of bands to justify this interpretation of the data (it is recognized that many bands may be too weak to be detected).

The fact that the visible-light photoproducts have the same absorptions for both CHD isomers makes us favor the idea of dehydrogenation to form Fe_2H_2 and benzene, as this is the only choice where the set of products would be common to both isomers

of CHD, as seen in Table V (the two insertion products, on the other hand, would be expected to have different absorptions due to the different arrangements of the C-C double bonds). It is interesting to note that in this case the dehydrogenation occurs via iron atoms and possibly dimers, whereas Morand and Francis attribute the CHD disproportionation to iron clusters.¹⁸ The idea presented here, that iron dimers dehydrogenate CHD, might be supported if other transition-metal dimers reacted in a similar way; such work is planned.

Conclusion

Iron and benzene have been shown to form at least three complexes in dilute argon matrices. These adducts have been identified as $\text{Fe}(\text{C}_6\text{H}_6)$, $\text{Fe}_2(\text{C}_6\text{H}_6)$, and $\text{Fe}(\text{C}_6\text{H}_6)_2$, where the relative amount of formation of each complex is dependent on the matrix reactant concentration. These results resolve any disagreements between previous research groups over the identification of the codeposition product being either the mono-(benzene)iron complex or the di(benzene)iron complex.

Iron atoms and dimers were seen to adduct with 1,3-CHD and 1,4-CHD, and upon photolysis with UV light the monoiron adducts rearranged to form $\text{Fe}(\text{C}_6\text{H}_6)$ and hydrogen in a dehydrogenation reaction. Since comparison of these results with similar reactions utilizing different transition-metal atoms will also be useful, similar studies with different metals are in progress.

Acknowledgment. The financial support of the National Science Foundation and the Robert A. Welch Foundation is greatly appreciated. Discussion of the iron-benzene results with Dr. W. Graham of the University of Alberta is acknowledged. Assistance with the synthesis and separation of cyclohexadiene- d_8 from Aki Kitamura and Greg Bodager is also greatly appreciated and acknowledged.

Supplementary Material Available: Infrared spectra of hydrogenated and deuterated cyclic C_6 hydrocarbons (2 pages). Ordering information is given on any current masthead.